DIAGNOSIS OF AZIMUTHAL SHEAR ASSOCIATED WITH TORNADOES

Travis Visco[1,2], Valliappa Lakshmanan[3,4], Travis M. Smith[3,4], Kiel L. Ortega[3,4]

[1]2009 National Weather Center Research Experiences for Undergraduates, Norman, Oklahoma

[2]State University of New York College at Oneonta, Oneonta, New York

[3]Cooperative Institute for Mesoscale Meteorology Studies, University Of Oklahoma, Norman, Oklahoma.

[4]NOAA/National Severe Storms Laboratory, Norman, Oklahoma.

Abstract

Current rotation detection algorithms are prone to poor performance due to high local variance in a Doppler radial velocity field. A new linear least squares derivatives (LLSD) technique has been developed which is less prone to problems from such variability and outputs a number of fields diagnosing the radial wind field, including azimuthal shear and radial convergence. We subjectively diagnosed rotation within thunderstorms from seven storm days which yielded eighty tornadoes. Threshold values and trends of azimuthal shear and radial convergence fields were extracted from the tornado producing storms. These values and trends will be used to train a new rotation-detection algorithm.

Introduction

Azimuthal shear is defined as the rotational derivative of radial velocity (Smith and Elmore 2004). Past rotation detection algorithms have not directly used azimuthal shear as a parameter (Stumpf et al. 1997) owing to the fact conventional techniques of calculating azimuthal shear from Doppler radial velocity has been prone to noisy and unrepresentative data (Smith and Elmore 2004). Using a new local, linear least squares derivative (LLSD) technique, it is possible to more accurately calculate radial velocity and pinpoint areas of rotation (Smith and Elmore 2004). By applying this new technique to velocity data from confirmed tornadoes it is possible to extract azimuthal shear and radial convergence to investigate the values and trends which are characteristic of a tornado.

1 Travis Visco, 4 Gale Lane Patchogue NY, 11772 visct65@oneonta.edu

Since the development of the LLSD algorithm, no research has explored the relationship between the values and trends of azimuthal shear and radial convergence, and tornadoes. These data are essential in the development of a new rotation and detection algorithm using the LLSD technique.

This manuscript explains the methods used to compare confirmed tornadoes to the azimuthal shear and radial convergence fields. The observed distribution and time trends of the fields will be presented, as well as examples of storms which confirm and refute the findings.

Methodology

We examined eighty tornadoes from seven different days, with tornado counts ranging from one tornado to thirty-nine tornadoes per day.

Azimuthal shear and radial convergence were

computed from radial velocity data from nearby WSR-88D radars using the LLSD technique of Smith and Elmore (2004).

Day	State(s)	Number of Tornadoes	Strongest Tornado
5 May 2007	Kansas	12	EF-5
7 January 2008	Illinois Michigan	3	EF-3
5 February 2008	Tennessee Mississippi	21	EF-4
22 May 2008	Colorado	1	EF-3
23 May 2008	Kansas Oklahoma	39	EF-4
25 May 2008	Iowa	3	EF-5
24 July 2008	New Hampshire	1	EF-2

Table 1: The Events Examined in This Study

The next step was to manually track areas of strong rotation that produced tornadoes. The center of rotation was identified by placing a marker in the center of the maximum azimuthal shear area on the lowest elevation scan (0.5 degrees). These points were then connected to form a track. The tracks were processed with the azimuthal shear and radial convergence fields in a software package which searched for the maximum in the two fields. The software started with a 5km search radius at the 0.5 degree tilt and expanded to a 7.5 km radius at the top tilt (19.5 degrees). The increase in search radius with elevation tilt was to account for storm motion. Figure 1 shows an example of the extraction technique.

The goal was to track the areas of strongest rotation from 30 minutes prior to the time when a tornado was confirmed through the end of the tornado. Not only is it important to gain knowledge on commonly observed values of azimuthal shear and radial convergence for tornadoes, but trends in those values prior to tornado formation could be important input in a rotation algorithm.

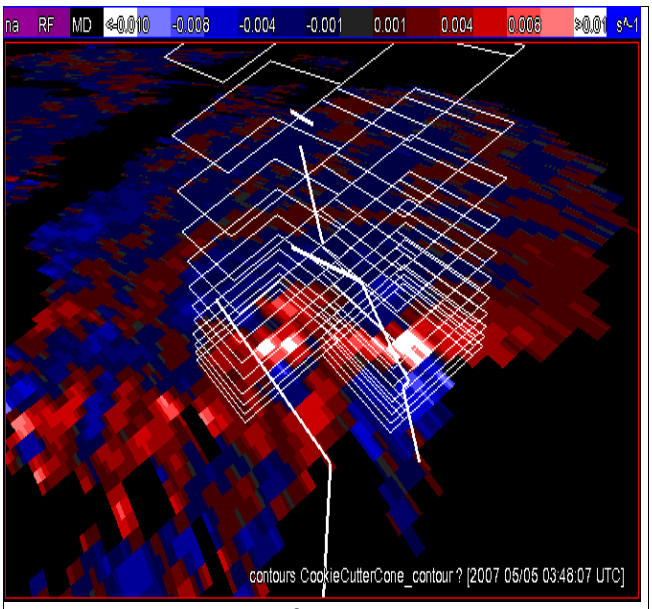

Figure 1: Depiction of azimuthal shear at 0.5 degree elevation showing two tornadic areas. The white boxes show the area where data will be extracted.

The extracted azimuthal shear and radial convergence values were plotted versus time relative to tornado formation. This revealed the azimuthal shear and radial convergence values at any time prior to or during the life of a tornado, as well as noticeable trends in the minutes leading up to tornado formation. Also, it made it possible to view all the tornadoes in the same frame of reference regardless of tornado duration.

Data from above 6km AGL and/or more than 150km from the radar were not used in any analysis. All of the storms were analyzed in two layer composites: 0 to 3 km AGL and 3 to 6 km AGL. A layer composite allowed for a broader depiction of storm characteristics, ensuring areas of strong circulation did not go unnoticed. The 3-6 km AGL layer was chosen to represent deep circulations associated with mesocyclones in long-lived supercell storms, while the 0-3 km AGL layer was chosen so that circulations near the ground that may not be as long-lived could be identified.

The distributions of the values are calculated for

five-minute intervals relative to each tornado's life cycle. All of the data points from each tornado were analyzed, and the maximum azimuthal shear and radial convergence values were retained . For example, if a radar scan had three elevations within the 0-3km AGL layer, then the elevation with the highest corresponding value of azimuthal shear or radial convergence would be retained to represent the tornado at that time. These maximum values were then combined and percentiles were calculated.

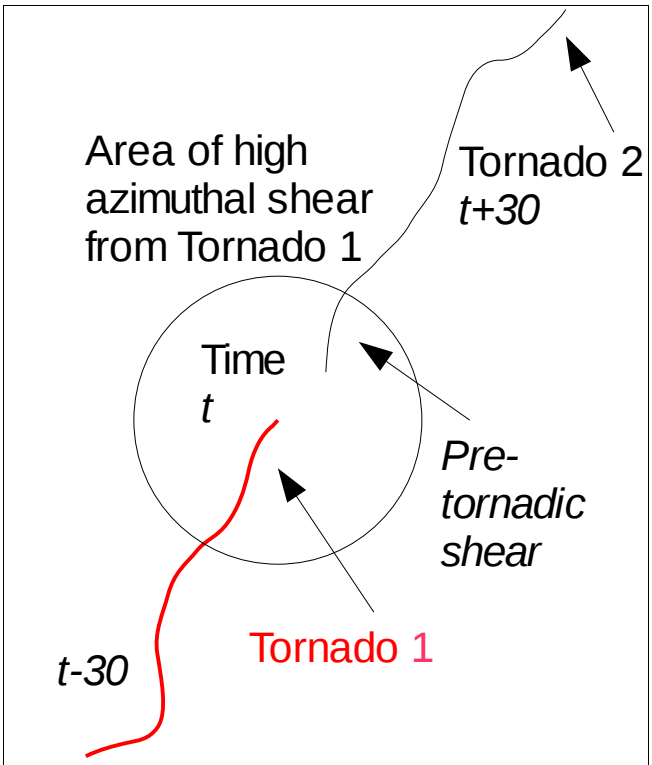

Figure 2: Multiple tornadoes sharing same area of high azimuthal shear

There was the need to prevent the values and trends from being skewed by multiple tornadoes forming from the same thunderstorm. For example, suppose tornado 1 has a start time of *t*, and tornado 2 has a start time of *t+30*. If the azimuthal shear values from tornado 2 were extracted as far back as 30 minutes prior to tornado formation, then those initial values for tornado 2 are actually the values associated with tornado 1. Thus, the initial values for tornado 2 are inflated and the trend is flattened. Figure 2 is a simple schematic of this problem. In order to avoid this problem, tornadoes which were the first to form from each thunderstorm were analyzed separately. Nineteen tornadoes in our data set were 'first tornadoes'.

The 'first tornado' data set was used to calculate the trends of azimuthal shear and radial convergence. These tornadoes were analyzed separately, then combined to reveal an average trend. Trends were calculated for azimuthal shear and radial convergence within the 0-3km AGL layer and the 3-6km AGL layer.

Results

A. *Lead Times and Distributions*

The goal of a forecaster is to issue a warning on 100% of tornadoes and with as much advanced warning as possible. By plotting values by percentiles, the value of azimuthal shear and radial convergence that corresponds to a certain percentage of tornadoes at a specific lead time can be discovered.

1. *Azimuthal Shear*

Figure 3 is a graph of the maximum azimuthal shear from the 0-3km AGL layer composite. The values from this graph were put into Table 2 to show what azimuthal shear values are representative of a specific percentage of tornadoes, relative to lead time. Time 0 is correspondent to the time the tornado forms. Tables like this would provide a quick and easy way for a forecaster to compare characteristics of a thunderstorm in real time with those of tornado-producing thunderstorms. In order to capture the majority of tornadoes, the azimuthal shear threshold would have to be set relatively low. Additionally, if an algorithm was tuned to only be concerned with high shear events (say greater than .017 s^{-1}), it would only detect about 25% of tornadoes.

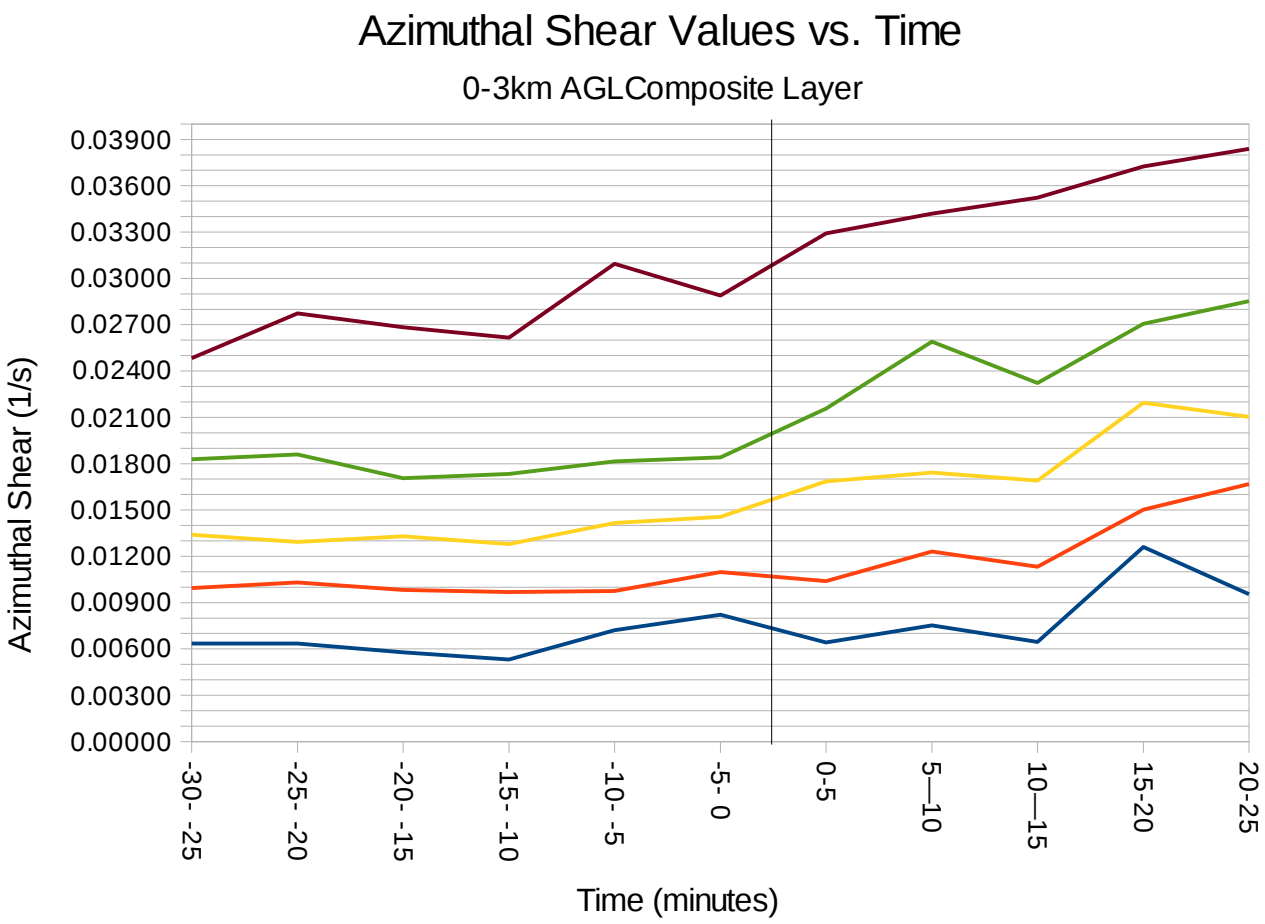

Figure 3: 0-3km AGL Layer Composite of Maximum Azimuthal Shear. This graph represents the maximum azimuthal shear (0-3km) of all eighty tornadoes, with respect to time. By breaking it down into percentiles, it is easily seen what ranges of values correspond to what percentage of tornadoes. The blue line represents the 5th percentile, the red line the 25th percentile, the yellow line the 50th percentile, the green line the 75th percentile and the brown line the 95th percentile. The vertical black line denotes the tornado start time.

Lead Time (min)	25% of tornadoes	50% of tornadoes	75% of tornadoes	95% of tornadoes
20	.01783	.01311	.01006	.00607
15	.01720	.01304	.00975	.00555
10	.01774	.01348	.00972	.00627
5	.01873	.01436	.01034	.00772
0	.01999	.01571	.01069	.00732
-5	.02374	.01714	.01135	.00697
-10	.02457	.01716	.01182	.00699

Table 2: 0-3km AGL Azimuthal Shear Layer Composite Percentiles and Lead Times

Figure 4 is a graph of the maximum azimuthal shear from the 3-6km AGL layer composite. Table 3 shows the azimuthal shear values at a specific lead time for a certain percentage of tornadoes.

As with the 0-3km AGL layer, the lower the value of azimuthal shear, the more tornadoes are captured.

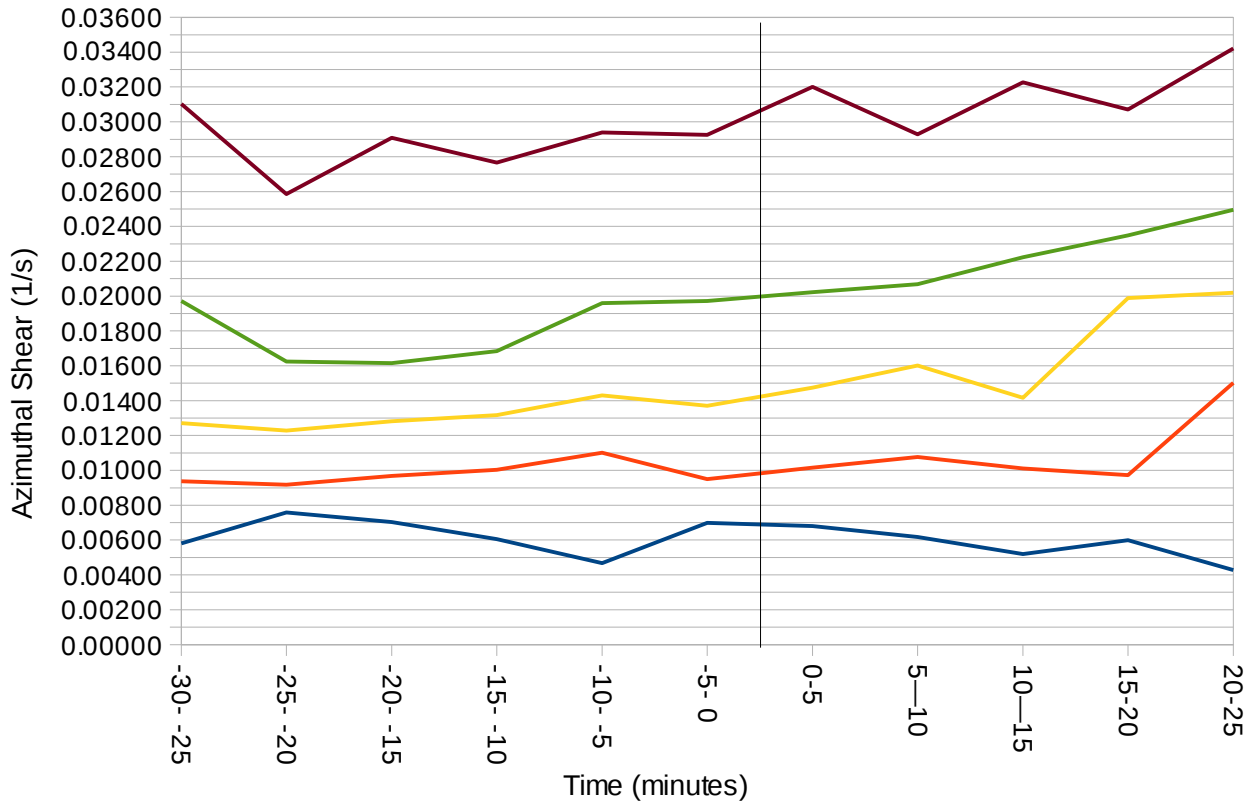

Figure 4: 3-6km AGL layer composite of maximum azimuthal shear. This graph represents the maximum azimuthal shear (3-6km) of all eighty tornadoes, with respect to time. The blue line represents the 5th percentile, the red line the 25th percentile, the yellow line the 50th percentile, the green line the 75th percentile and the brown line the 95th percentile. The vertical black line denotes the tornado start time.

Lead Time (min)	25% of tornadoes	50% of tornadoes	75% of tornadoes	95% of tornadoes
20	.01621	.01255	.00943	.00731
15	.01651	.01300	.00986	.00654
10	.01822	.01374	.01052	.00537
5	.01965	.01401	.00975	.00583
0	.01997	.01423	.00983	.00690
-5	.02046	.01539	.01046	.00650
-10	.02146	.01510	.01044	.00569

Table 3: *3-6km AGL Azimuthal Shear Layer Composite Percentiles and Lead Times*

From these tables, it becomes possible to decide on a threshold for azimuthal shear that would capture a certain percentage of tornadoes.

2. Radial Convergence

Another output from the LLSD technique is radial convergence. Only the 0-3km AGL layer was analyzed. Figure 5 is a graph of the maximum radial convergence from the 0-3km AGL layer composite.

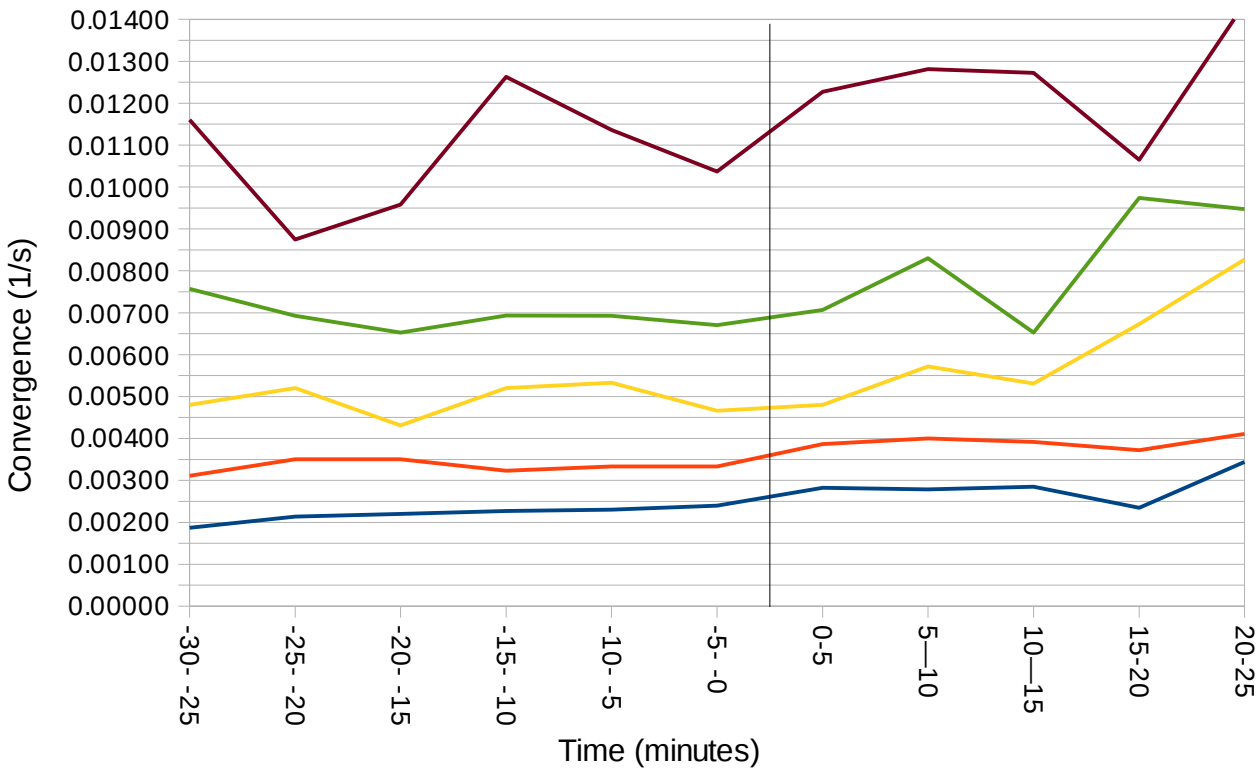

Figure 5: 0-3km AGL Radial Convergence. This graph represents the maximum convergence (0-3km layer) of all eighty tornadoes, with respect to time. The blue line represents the 5th percentile, the red line the 25th percentile, the yellow line the 50th percentile, the green line the 75th percentile and the brown line the 95th percentile. The vertical black line denotes the tornado start time.

Lead Time (min)	25% of tornadoes	50% of tornadoes	75% of tornadoes	95% of tornadoes
20	.00670	.00476	.00351	.00217
15	.00674	.00476	.00335	.00224
10	.00694	.00527	.00328	.00229
5	.00682	.00500	.00333	.00235
0	.00689	.00474	.00360	.00262
-5	.00769	.00526	.00394	.00281
-10	.00742	.00552	.00396	.00282

Table 4: 0-3km AGL Radial Convergence Composite Layer Percentiles and Lead Times

The values from this graph were put into Table 4 to show what convergence values are representative of a specific percentage tornadoes, relative to lead time. Time 0 is correspondent to the time the tornado forms.

B. Trends

The second aspect of recognizing potential tornado formation is the trends in the azimuthal shear and radial convergence values in the minutes prior to tornado formation. By analyzing the nineteen tornadoes that were the first to form from each thunderstorm, useful trends were discovered.

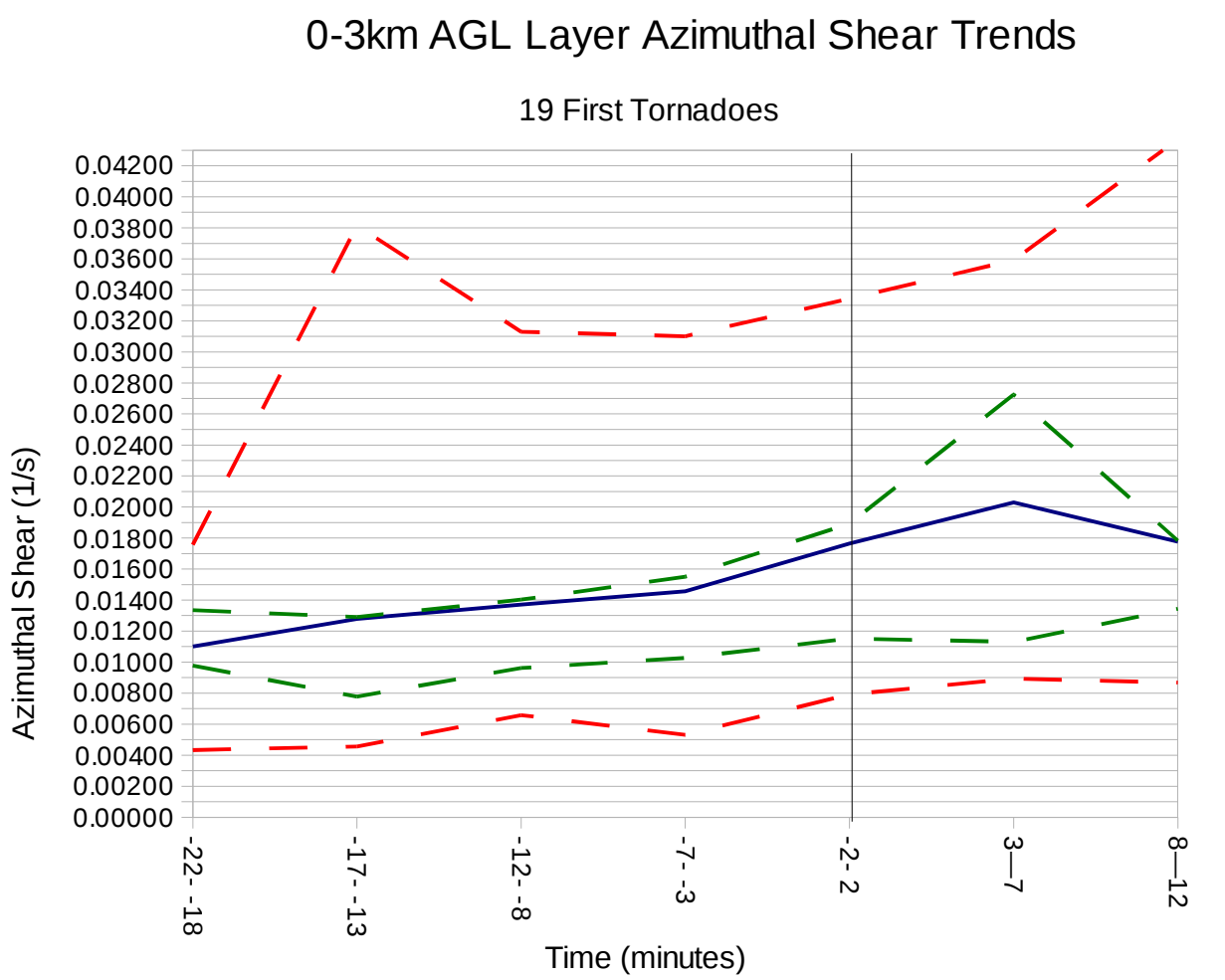

Figure 6: Trends of 0-3km AGL layer composite maximum azimuthal shear. This graph shows the average 0-3km azimuthal shear trend of the 19 tornadoes that were the first to form from each thunderstorm. The blue line is the average trend, the red dashed lines are the minimum and maximum values, and the green dashed lines are the 33% confidence intervals. The vertical black line represents the tornado start time.

1. *Azimuthal Shear*

Figure 6 is a plot of the average trend of maximum azimuthal shear in the 0-3km AGL composite layer for all nineteen 'first tornadoes'. Table 5 shows the average difference in azimuthal shear in 5 minute increments. The difference at a particular time represents the difference in shear from 5 minutes prior, until that time. For the 0-3km AGL layer, the 10 minutes leading up to tornado formation saw the average azimuthal shear increase from .01371 s^{-1} to .01765 s^{-1}, for an increase of .00394 s^{-1}. Also, the biggest increase in shear between each 5-minute interval occurred in the 5 minutes before tornado formation (0 minute lead time in table), with an average increase of .00309 s^{-1}.

Lead Time (min)	Average Difference in Azimuthal Shear
15	.00178
10	.00093
5	.00086
0	.00309
-5	.00265
-10	-.00254

Table 5: Average Difference in 0-3km AGL layer Azimuthal Shear

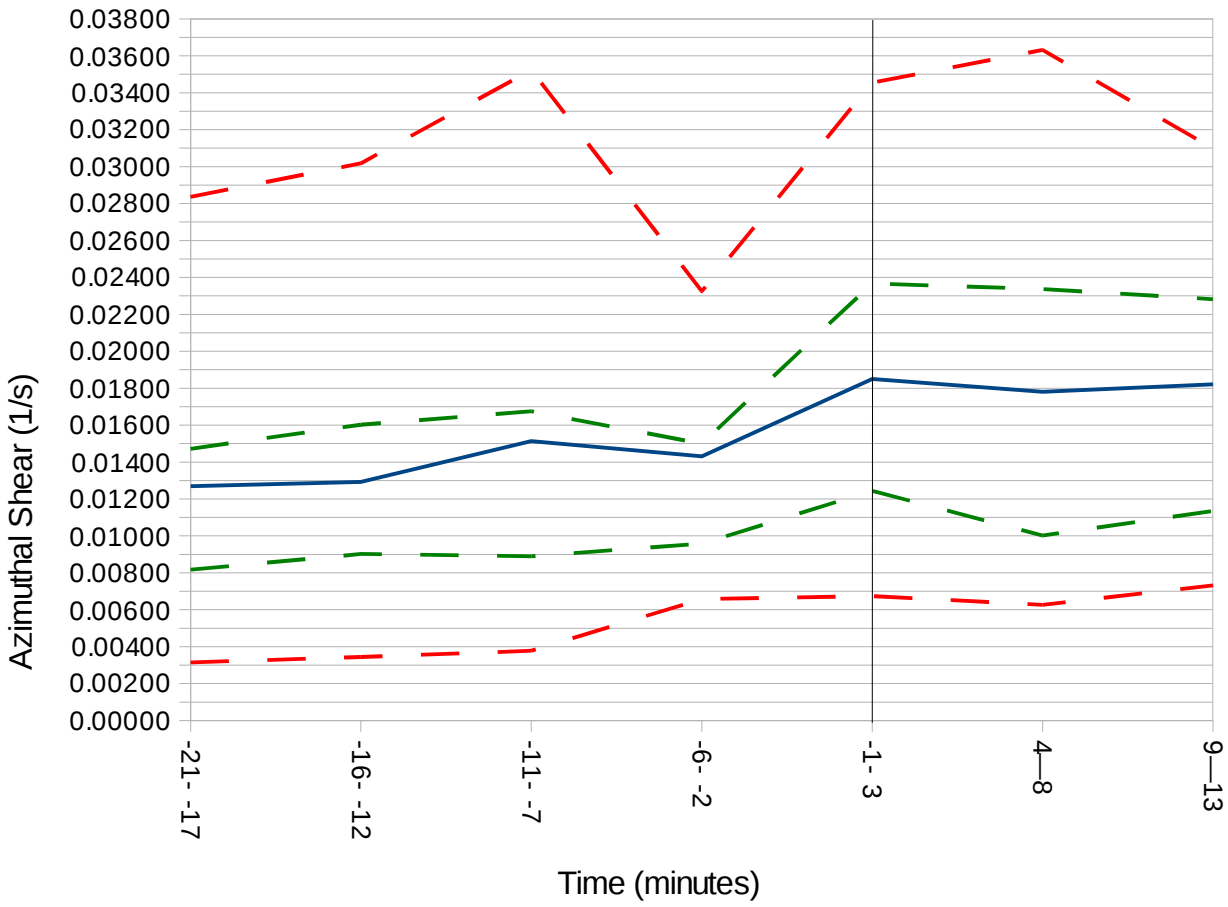

Figure 7: Trends of 3-6km AGL layer composite maximum azimuthal shear. This graph shows the average 3-6km azimuthal shear trend of the 19 tornadoes that were the first to form from each thunderstorm. The blue line is the average trend, the red dashed lines are the minimum and maximum values, and the green dashed lines are the 33% confidence intervals. The vertical black line represents the tornado start time.

Figure 7 is a plot of the average trend of maximum azimuthal shear in the 3-6km AGL composite layer for all nineteen 'first tornadoes'. Table 6 shows the 5 minute average difference in azimuthal shear. For the 3-6km AGL layer, the 10 minutes leading up to tornado formation saw shear increase from .01514 s^{-1} to .01850 s^{-1}, for an increase of .00336 s^{-1}. Again, the largest increase occurred in the 5 minutes prior to tornado formation (0 minute lead time in table), with the average increase being .00419 s^{-1}. Although slight, there was a decrease in shear values from 10 minutes prior to tornado formation, to 5 minutes prior to formation (5 minute lead time in table).

Lead Time (min)	Average Difference in Azimuthal Shear
15	.00024
10	.00221
5	- .00083
0	.00419
-5	- .00069
-10	.00040

Table 6: Average Difference in 3-6km AGL Layer Azimuthal Shear

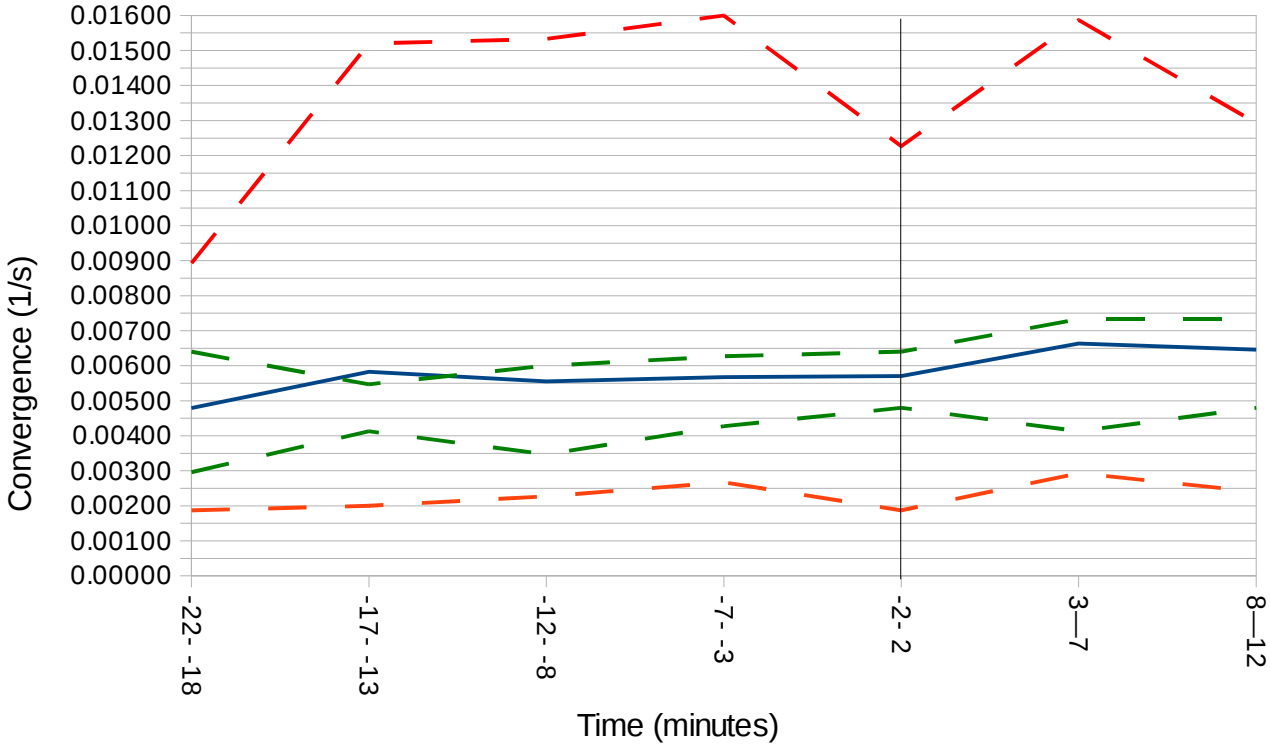

Figure 8: Radial Convergence Trends. This graph shows the average 0-3km layer convergence trend of the 19 tornadoes that were the first to form from each thunderstorm. The blue line is the average trend, the red dashed lines are the minimum and maximum values, and the green dashed lines are the 33% confidence intervals. The vertical black line represents the tornado start time.

2. Radial Convergence

Using the nineteen 'first tornadoes', average trends in radial convergence were plotted (Figure 8). While the values of radial convergence were about an order of magnitude less than those of azimuthal shear, there is still a slight increasing trend in values from tornado start time, to 5 minutes into tornado life. Other than that time period, the graphs show no significant increase. Additionally, it can be seen the distributions are greatly skewed towards lower values of radial convergence.

C. *Maximum and Minimum Azimuthal Shear and Radial Convergence Values*

It is also useful to see what the lowest and highest azimuthal shear and radial convergence values were, in order to gain perspective on the range for most tornadoes. Of the eighty tornadoes, the lowest azimuthal shear value observed from the 0-3km AGL layer during the actual tornado was .00370 s^{-1}, while the highest was .05137 s^{-1}. For the 3-6km AGL layer, the lowest observed value was .00311 s^{-1}, and the highest was .04488 s^{-1}.

For radial convergence, the lowest observed value from the 0-3km AGL layer during a tornado was .00120 s^{-1}, while the highest was .02467 s^{-1}.

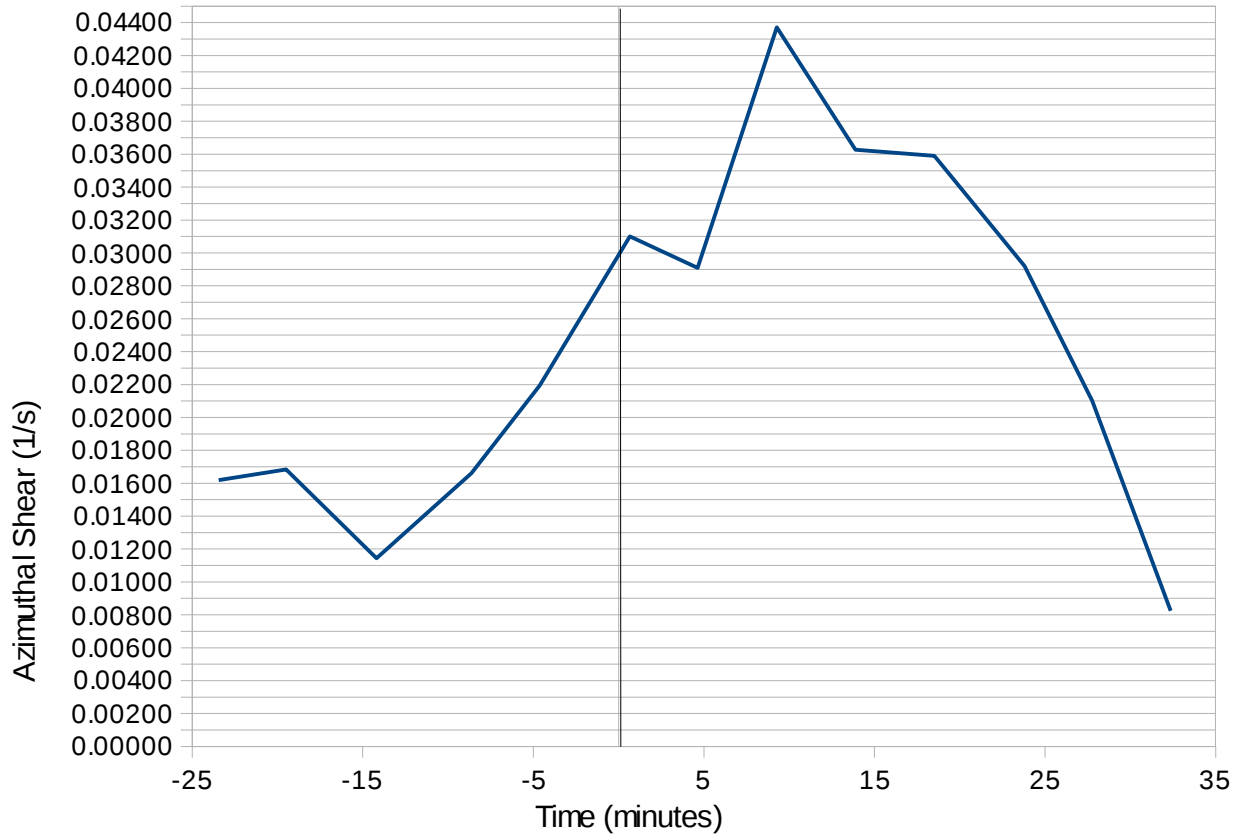

Figure 9: This graph is from a tornado that supports the azimuthal value and trend findings of this study. The blue line is the maximum azimuthal shear (0-3km AGL layer) over time, and the vertical black line represents tornado start time. There is a strong increasing trend observed starting 15 minutes prior to tornado formation.

D. Supportive Case : 23 *May 2008*

This particular day saw thirty-nine tornadoes, nine of which were 'first tornadoes'. One of these serves as a example of a tornado which illustrated high values of azimuthal shear, as well as a strong increasing trend. This tornado had one of the highest shears of any of the eighty looked at (0-3km AGL max shear of .04371 s^{-1} 9 minutes into tornado life). Figure 9 shows the azimuthal shear (0-3km AGL layer) rapidly increasing from 15 minutes prior to tornado formation, until 9 minutes into the tornado's life. The increase in the 10 minutes prior to formation was .015 s^{-1}, which is significantly higher than the computed average. The trends from the 3-6km AGL composite layer follow suit, with the maximum shear occurring 10 minutes after tornado formation, with a value of .0488 s^{-1}. Further, in the 10 minutes prior to tornado formation, the increase in azimuthal shear was .017 s^{-1}, again well above the noted average.

E. Non-Supportive Case: 23 *May 2008*

There was a confirmed tornado which counters the calculated average of azimuthal shear trends. Figure 10 shows the 0-3km AGL layer azimuthal shear is at a maximum 5 minutes before the

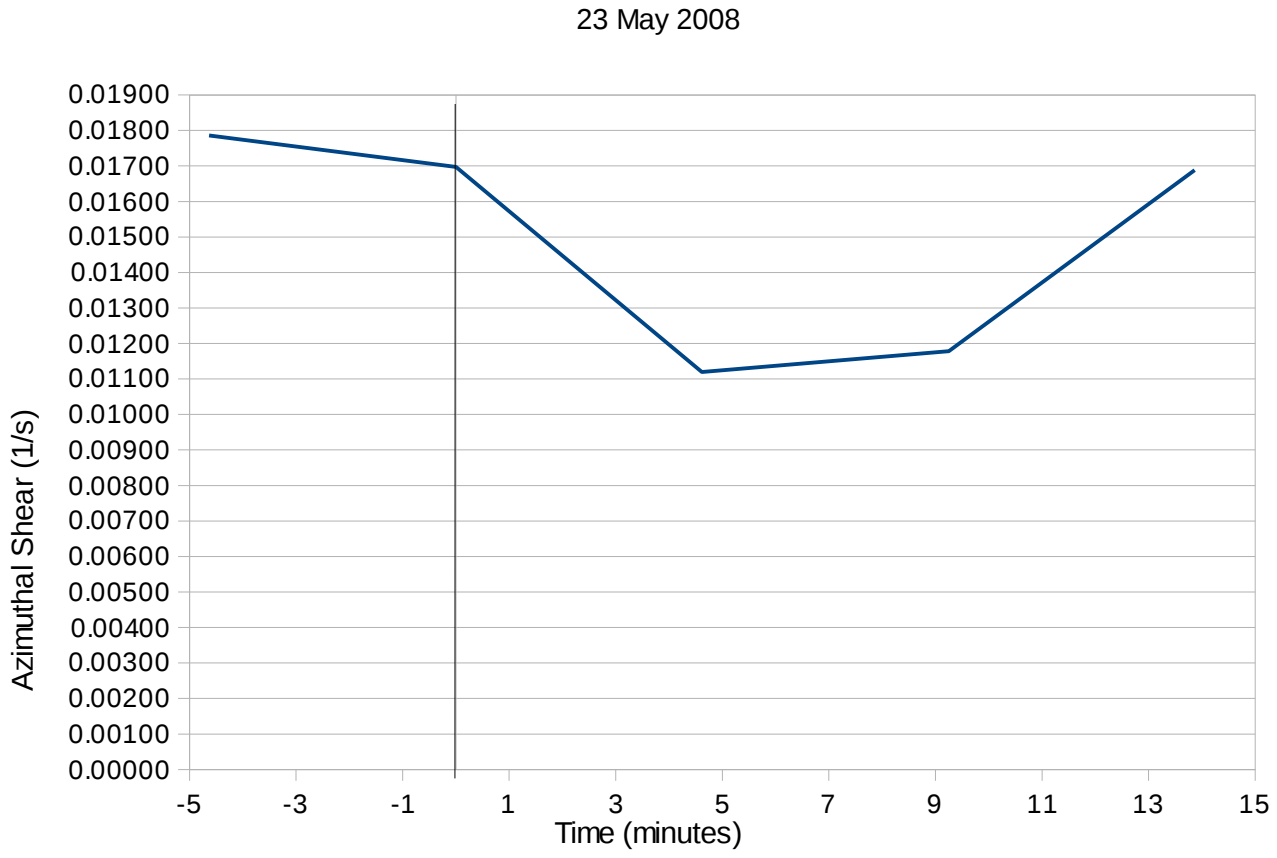

Figure 10: This graph is from a tornado that does not support the azimuthal trend findings of this study. The blue line is the maximum azimuthal shear (0-3km AGL layer) over time, and the vertical black line represents tornado start time.

tornado formed, and then steadily decreases for the majority of the tornado's life. While its lowest azimuthal shear value (.01120 s^{-1} 5 minutes after tornado formation) is a value indicative of 75% of tornadoes, the decreasing trend goes against the average increasing trend. In the 10 minute time span from 5 minutes prior to tornado formation until 5 minutes after formation, the azimuthal shear decreases by .00666 s^{-1}. The shear in the 3-6km AGL layer level also decreases for the first 6 minutes of the tornado's life, before increasing. The minimum value of azimuthal shear observed from this tornado from 3-6km AGL was .01002 s^{-1}.

Conclusion

The goal of this study was to explore the values and trends of azimuthal shear and radial convergence associated with tornadoes. Important values and trends in azimuthal shear and radial convergence have been discovered for tornadoes by analyzing eighty tornadoes.

It was found that azimuthal shear and radial convergence values have a large spread in the distribution for tornadoes. In order to capture most tornadoes, the value of azimuthal shear and radial convergence would have to be set relatively low. The azimuthal shear and radial convergence values of 95% of tornadoes is less

than half the value 50% of tornadoes have.

In addition to specific values of azimuthal shear and radial convergence, exploring trends in azimuthal shear and radial convergence is important for training a new rotation detection algorithm. For azimuthal shear, the 5 minute window prior to tornado formation contained the highest increase in shear values at both the 0-3km AGL and 3-6km AGL layers, based off the nineteen 'first tornadoes'. Radial convergence however did not show any strong trends before tornado formation, and only a slight increasing trend in the 5 minutes after tornado formation.

It should be noted that azimuthal shear and radial convergence were extracted from the velocity data by the LLSD technique using the same settings. The settings ideal for azimuthal shear may not be the same as the settings ideal for radial convergence. Further work with exploring different settings will need to completed.

This research was the first step in a larger project to train a new rotation detection algorithm. Research needs to be done on non-tornadic cases in order to find a distinction between the two. The values and trends of azimuthal shear and radial convergence that capture the greatest percentage of tornadoes, yet a small percentage of non tornado producing thunderstorms, will serve as parameters for the new rotation detection algorithm. Additionally, future work will be done to explore the use of other outputs, such as LLSD-derived gate-to-gate velocity difference, and their skill in detecting tornadoes.

Acknowledgments

This material is based upon work supported by the National Science Foundation under Grant No. ATM-0648566. Any opinions, findings, and conclusions or recommendations expressed in this material are those of the author(s) and do not necessarily reflect the views of the National Science Foundation.

References

Smith, T.M., and K.E. Elmore, 2004: The Use of Radial Velocity Derivative to Diagnose Rotation and Divergence. Preprints, The 11th Conference on Aviation, Range, and Aerospace and the 22nd Conference on Severe Local Storms, Hyannis MA, American Meteorological Society

Stumpf, G.J., A. Witt, E.D. Mitchell, P.L. Spencer, J.T. Johnson, M.D. Eilts, K.W. Thomas, and D.W. Burgess, 1997: The National Severe Storms Laboratory Mesocyclone Detection Algorithm for the WSR-88D. *Weather and Forecasting, **13**, pp. 304-326*